

Organic & Biomolecular Chemistry

Accepted Manuscript



This is an *Accepted Manuscript*, which has been through the Royal Society of Chemistry peer review process and has been accepted for publication.

Accepted Manuscripts are published online shortly after acceptance, before technical editing, formatting and proof reading. Using this free service, authors can make their results available to the community, in citable form, before we publish the edited article. We will replace this *Accepted Manuscript* with the edited and formatted *Advance Article* as soon as it is available.

You can find more information about *Accepted Manuscripts* in the [Information for Authors](#).

Please note that technical editing may introduce minor changes to the text and/or graphics, which may alter content. The journal's standard [Terms & Conditions](#) and the [Ethical guidelines](#) still apply. In no event shall the Royal Society of Chemistry be held responsible for any errors or omissions in this *Accepted Manuscript* or any consequences arising from the use of any information it contains.

Rational Design of Catalysts for Asymmetric Diamination Reaction using Transition State Modeling

Garima Jindal and Raghavan B. Sunoj*

Department of Chemistry, Indian Institute of Technology Bombay, Powai, Mumbai 400076

sunoj@chem.iitb.ac.in

Abstract

The stereoselective synthesis of 1,2-diamines has remained a formidable challenge. A recent palladium-catalyzed asymmetric diamination of conjugated double bonds by using di-*tert*-butyldiaziridinone appears promising. The axially chiral binol phosphoramidite ligands are successful in offering high enantioselectivity. The density functional theory investigations revealed that the energies of the stereocontrolling transition states for the C-N bond formation depend on a number of weak non-covalent interactions such as C-H \cdots π , C-H \cdots O and anagostic interactions. We envisaged that the modulation in these interactions in the transition states, through subtle changes in chiral phosphoramidite substituents could be exploited toward steering the stereoselectivity. The effect of systematic modifications on both 3,3' positions of the binol as well as on the amido nitrogen on the stereochemical outcome is predicted. It is identified that high enantioselectivity requires a balance between the nature of the substituents on binol and amido groups. Reduced size of the amido substituents demands increased bulk on the binol whereas lowering the size on the binol demands increased bulk on the amido for higher stereoselectivity. The substituent at the α -position of the amido group is found to be vital and appears to be a hot spot for modifications. These insights derived through studies on the stereocontrolling transition

states could help improve the catalytic efficacies in palladium-catalyzed asymmetric diamination reactions.

Introduction

The design of chiral ligands has remained in the forefront of chemical research in asymmetric catalysis for decades.¹ The ever-increasing predictive power of modern computational chemistry tools in concert with mechanistic understanding is now being perceived as a potentially important strategy in the design of asymmetric catalysts.² Emerging trends indicate that computational methods are increasingly being employed for designing new catalysts, ranging from small molecules to artificial enzymes.³ In particular, the predictions on mechanisms and stereoselectivities on a plethora of reactions have been found to be in excellent mutual agreement.⁴ Rational predictions in catalysis appear to hold potential toward minimizing the tedious and occasionally time consuming trial and error loops of experimentation.⁵

The computational design of an entirely new class of catalyst is a formidable challenge as large differences in the nature of the substrate and/or catalysts could lead to unpredictably large mechanistic variations. However, the design of newer catalysts for the same genre of reactions with a certain degree of structural similarity is likely to be more successful. Computational design of asymmetric catalysts would typically demand knowledge on the reaction mechanism as well as on the stereocontrolling event(s).⁶ Such protocols for catalyst design have been employed in both organocatalysis and organometallic catalysis. For instance, Houk and coworkers have reported the design of a new Rh-catalyzed Diels-Alder reactions.⁷ We, as well as others, have designed proline based organocatalysts for aldol^{4b,6a,8} and Mannich reaction.^{6d} The experimental verification of the effectiveness of such catalysts was subsequently reported and was found to be in agreement with the predictions.⁹ Goddard and coworkers proposed an Ir-N-heterocyclic catalyst for the

hydroxylation of methane,¹⁰ which was found to be successful in the experimental studies that ensued.^{3c} In another interesting study, Schoenebeck and coworkers employed a combined computational and experimental approach to revert the selectivity in a Pd-catalyzed cross coupling reaction.¹¹ In all these approaches, the knowledge on the transition states that are responsible for the stereoselectivity and/or that controls the rate of the reaction is vital to the success of rational modifications to asymmetric catalysts.

In continuation with our long-standing interest in understanding the origins of asymmetric induction,¹² very recently we have established the mechanism of a palladium catalyzed asymmetric diamination reaction in the presence of a chiral phosphoramidite ligand.¹³ Asymmetric diamination is a relatively newer and promising class of reaction belonging to the family of double bond functionalization reactions such as asymmetric dihydroxylation or aminohydroxylations.¹⁴ The synthesis of vicinal diamines is important due to the presence of such functionalities in natural products, biologically active compounds and also in chiral ligands.¹⁵ The reaction, as summarized in Figure 1, employs di-*tert*-butyldiaziridinone as the nitrogen source and chiral phosphoramidite as a ligand for palladium. The experimentally observed enantioselectivities in favor of the *trans*-diamines have been reported to depend on the nature of the chiral phosphoramidite used in the reaction. The synthesis of vicinal diamines is a challenging problem and there are only a few examples wherein excellent stereoselectivities have been reported.^{14a} The use of monodentate phosphoramidites, with a chiral binol and an amido group, have been successful in inducing chirality (Figure 1).¹⁶ While in most cases the source of chirality is due to an axially chiral binol motif, examples wherein the amido group bears chiral carbon atoms are also reported.¹⁷ In this article we intend to disclose a rational approach, aided by

transition state modeling, toward designing improved catalysts for an asymmetric diamination reaction.

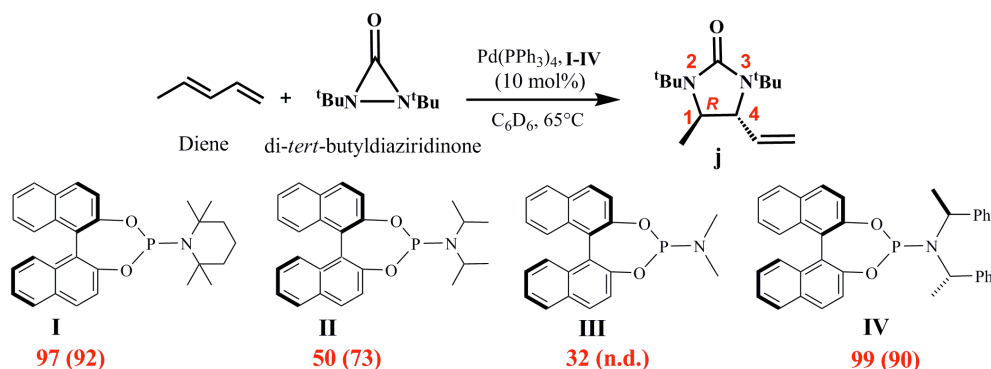


Figure 1. Pd-*tetrakis*-(triphenyl)phosphine-catalyzed diamination of conjugated dienes by di-*tert*-butyldiaziridinone in the presence of chiral phosphoramidites. The computationally predicted *ees* at the B3LYP level of theory are provided together with the experimental values in parenthesis (refs.13 and 16).

Computational Methods

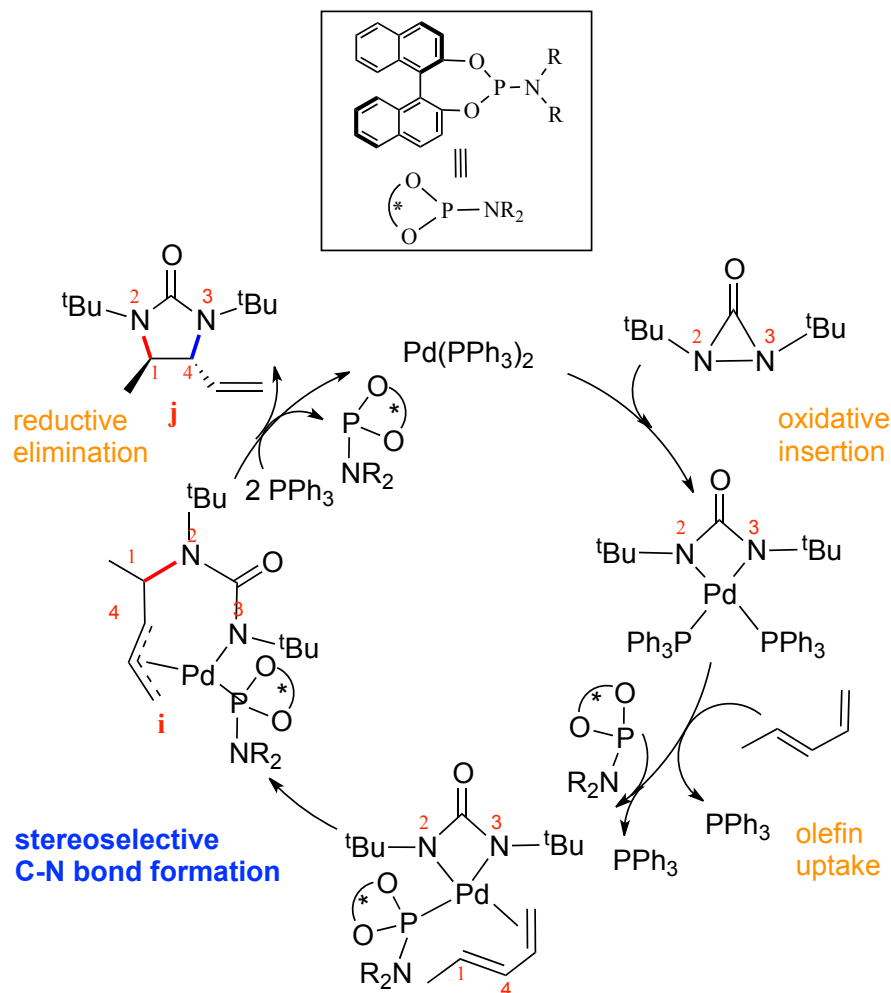
All calculations were done using GAUSSIAN 09 program.¹⁸ The hybrid density functional theories such as the B3LYP and the M06 were used for geometry optimization (catalysts **I-IV**) with 6-31G* basis set for all atoms except Pd.¹⁹ For Pd atom, LANL2DZ basis set with effective core potential (ECP) was used.²⁰ The stationary points were characterized by frequency calculations. Single point calculations were further performed with the M06 functional using 6-31G** as the basis set for all other atoms except Pd, for which LANL2DZ is used. The empirical dispersion correction for the B3LYP functional, i.e., B3LYP-D method, is also used for calculating the energetics for all catalysts.²¹ The Gibbs free energies in all cases were calculated by adding the thermal corrections obtained at the level of theory at which optimization is carried out. Topological analysis of the electron densities within Bader's Atoms-in-Molecule (AIM)

framework was carried out by using AIM2000 software.²² The electron density (ρ_{bcp}) at the bond critical point (bcp) along the bond path is proportional to the strength of the bond (or other interactions present between two atoms) in a given molecule. There are a number of reports wherein the quantification of noncovalent interactions such as a C-H \cdots π interaction has been done using the AIM analysis.²³ The average ρ_{bcp} value for weak noncovalent interactions lies in the range of 0.020-0.002 a.u.

The transition state nomenclature used in this article includes the catalyst number followed by the prochiral face (*re* or *si*) of the approaching diene.

Results and Discussions

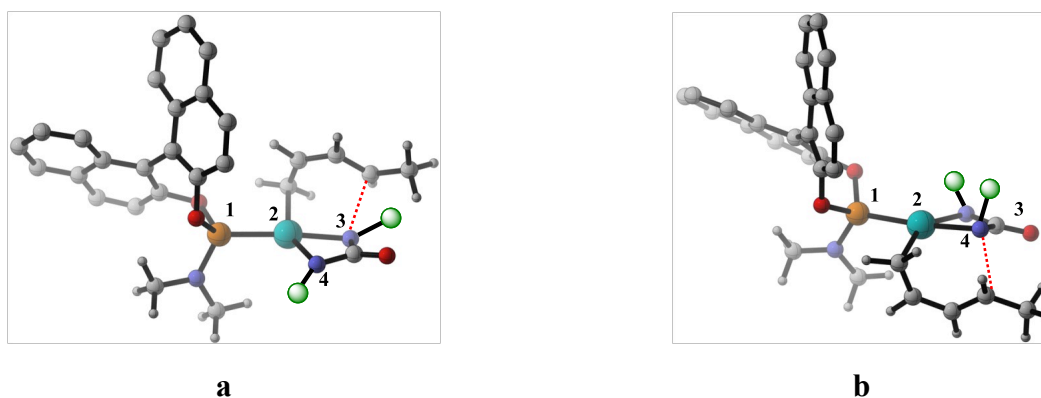
The mechanism can broadly be envisaged to involve the key steps as shown in Scheme 1. Initially, the palladium *tetrakis* complex dissociates to the *bis* complex so that the substrates can coordinate. The oxidative insertion of palladium to the N-N bond of diaziridinone is the first important step. The ensuing exchange of the neutral triphenylphosphine ligands by the diene and the chiral phosphoramidite sets stage for the first stereoselective C-N bond formation. The intermediate thus formed can undergo reductive elimination wherein the second C-N bond formation takes place to furnish the product. In the final product two chiral centres are formed. The first C-N bond formation leading to the formation of intermediate **i** controls the enantioselectivity and the second one leading to the final product **j** decides the diastereoselectivity. In the present article the emphasis is placed on the enantioselectivity controlling step.



Scheme 1. Mechanism of Pd-*bis*-(triphenyl)phosphine-catalyzed diamination of conjugated dienes by di-*tert*-butyldiaziridinone.

The stereocontrolling step for asymmetric diamination reaction described above has been identified as the C1–N2 bond formation between the diene and the diaziridinone nitrogen.¹³ More importantly, the stereoelectronic analysis of the diastereomeric transition states indicated that subtle differences in the weak interactions exert a direct and noticeable impact in stereoselection. Herein, we illustrate how modest and systematic variations in the catalyst framework can lead to large changes in its ability to induce improved stereoselectivity.

Among the different axially chiral catalysts examined experimentally, only **I** and **IV**, as shown in Figure 1, offered high enantioselectivity. It is prudent to note that the computational prediction of enantiomeric excess for these catalysts are in good agreement with the experimental observation.¹³ The enantio- and diastereo-selectivities respectively depend on the C1-N2 and C4-N3 bond formation, wherein new chiral centers are generated. The extent of enantioselectivity is computed on the basis of the energy difference between the competing diastereomeric transition states. Each of these transition states are identified after a fairly rigorous consideration of various stereochemical possibilities. Different possible modes of approach of the diene to the catalyst, designated as **a** – **d** in Figure 2, differ in the orientation of the diene with respect to the P(1)-Pd(2)-N(3)-N(4) plane of the catalyst. In modes **a** and **d**, the diene approaches from the rear side while in **b** and **c** the diene attacks from the front face. In each of these modes, the approach of both the *re* and *si* prochiral faces of the diene are considered as well. Thus, a total of 8 important stereochemical possibilities are examined in the stereocontrolling transition state. In each of these stereochemical modes, additional conformers arising as a result of the changes in the orientations of the amido substituents are also considered so as to identify the lowest energy transition state.²⁴



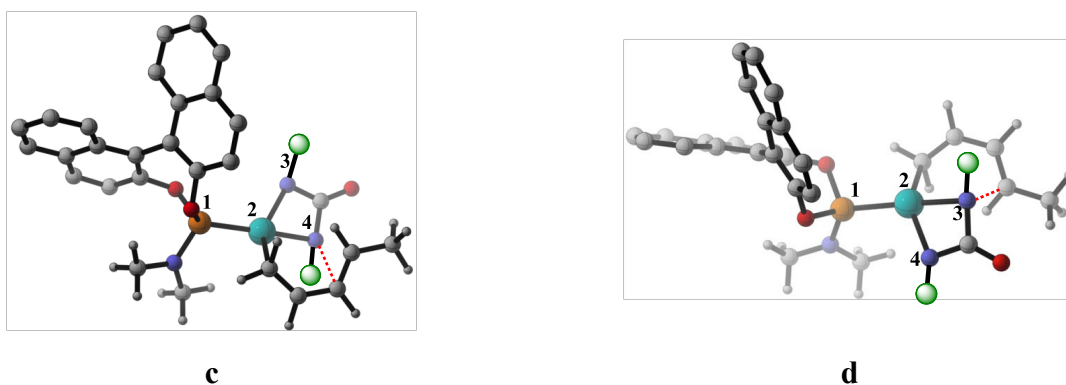


Figure 2. Different modes of approach of diene through *re* face for a representative case (catalyst **III**).

Table 1. Comparison of Computed and Experimental *ees* for Catalysts **I** – **IV** at Different Levels of Theory (L1-L5)^a

Catalyst	%ee					
	L1	L2	L3	L4	L5	Experimental
I	97	99	>99	99	>99	91
II	50	92	73	47	69	73
III	33	98	64	40	77	n.d.
IV	99	77	95	97	91	90

^a L1=B3LYP/6-31G*,LANL2DZ(Pd), L2=M06/6-31G*,LANL2DZ(Pd), L3= M06/6-31G**,LANL2DZ(Pd)//B3LYP/6-31G*,LANL2DZ(Pd), L4=SMD_(Benzene)/M06/631G**,LANL2DZ(Pd)//B3LYP/6-31G*,LANL2DZ(Pd), L5= B3LYP-D/6-31G**,LANL2DZ(Pd)//B3LYP/6-31G*,LANL2DZ(Pd).

First, geometry optimization of the transition states are performed by using both the B3LYP and the M06 functionals for the experimentally known catalysts **I** – **IV**. A comparison of the computed enantioselectivities obtained at various levels of theory and the corresponding experimental values (Table 1) indicates that the trends remain the same at both the B3LYP and

M06 levels of theory. More importantly, the predicted enantioselectivities are generally in good agreement with the experimental values. The predicted selectivities computed by using the energies at the M06 (L4) and B3LYP-D (L5) functionals by way of single point energies on the B3LYP geometries, appear to offer values quantitatively closer to the experimental enantioselectivities. For instance, the experimental studies by Shi and co-workers demonstrated that catalysts **II** and **III** yield only low *ee*.¹⁶ However, the *ees* are found to be overestimated, when computed using the energies of fully optimized transition state geometries at the M06 level of theory.¹³ In a recent review, Goodman and co-workers have recommended the use of single-point energies using the meta-GGA functionals on the B3LYP geometries for near-quantitative predictions of enantioselectivities. The analysis of the geometric features of the diastereomeric transition states obtained at the M06 level of theory appears to indicate that the weak C-H \cdots π interactions in the lower energy TS are overestimated. An instructive comparison of the vital weak interactions in transition state **III-re** is valuable at this juncture. It can be seen from Figure 3 that the C-H \cdots π contact distance reduces from 3.32 Å at the B3LYP (**III-re**) to 2.98 Å at the M06 (**III-re-M06**) level of theory. Interestingly, other weak interactions such as the anagostic and C-H \cdots O remain almost similar at both these levels of theory. Since the C-H \cdots π interaction is present only in the lower energy transition state **III-re**, the overestimation of the same at the M06 functional could be regarded as responsible for the larger energy difference between the diastereomeric transition states. This situation leads to overestimation of the predicted enantiomeric excess. A similar situation leading to an overestimation of C-H \cdots π interaction at the M06-2X level of theory and the accompanying overestimation of the *ee* has been noticed earlier by Houk and coworkers as well.²⁵ In another example, involving an N-heterocyclic carbene catalyzed [4+2] cycloaddition between a ketene and N-benzoyldiazene, the M05-2X functional

resulted in incorrect stereoselectivity as compared to the experimental observation.²⁶ On the basis of (a) the excellent agreement between the computed and experimental selectivities as well as (b) the literature reports on enantioselective reactions, we have employed the M06/6-31G**//B3LYP/6-31G* level of theory for the design of new asymmetric catalysts for diamination reaction.

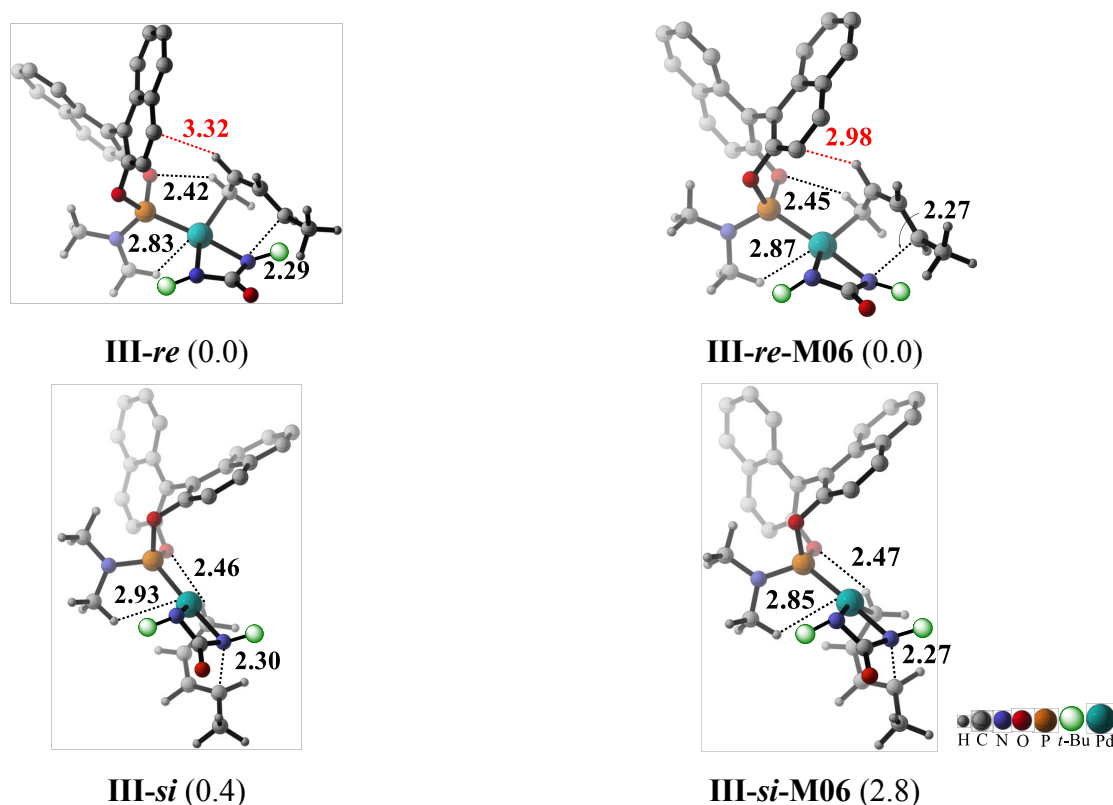


Figure 3. Optimized geometries of the lowest energy transition states for catalyst **III** at the B3LYP and M06 levels of theory. The relative energies (kcal/mol) in each case are provided in parenthesis. All distances are in Å.

A closer examination of the efficiency of the experimentally known catalysts reveals that the variations in the amido substituents exerts a pronounced effect on the stereochemical outcome of the reaction. In line with this observation, our transition state models for the stereocontrolling step have also identified that the steric bulk on the amido group of the catalyst is vital in dictating

the relative energies.¹³ Among the available class of phosphoramidites, modifications of substituents at the 3,3' position of the binol framework is relatively less common for asymmetric reactions.²⁷ Both structural and electronic modifications at the amido as well as binol groups have been attempted and their relative efficiencies are evaluated. The experimentally observed product, which is the *R* stereoisomer, can be formed by the approach of the *re* face of the diene to the diaziridinone nitrogen (Figure 1). The condition for the formation of the *R* enantiomer is that the transition state for the approach of the *re* face of the diene to the diaziridinone nitrogen should be of lower energy (Figure 1).

To begin with, the effect of varying the binol 3,3' substituents is examined by keeping the dimethyl amido group the same as in one of the experimentally known catalysts **III**. Since, the methyl groups offer least steric bulk, the present series of ligands would help ascertain the modulations in stereoselectivity the binol substituents are capable of imparting. In this group of catalysts, the key modifications are therefore done with the binol 3,3' substituents. The correlations between the computed *ees* and the nature of binol 3,3' substituents can be gleaned from Figure 4.

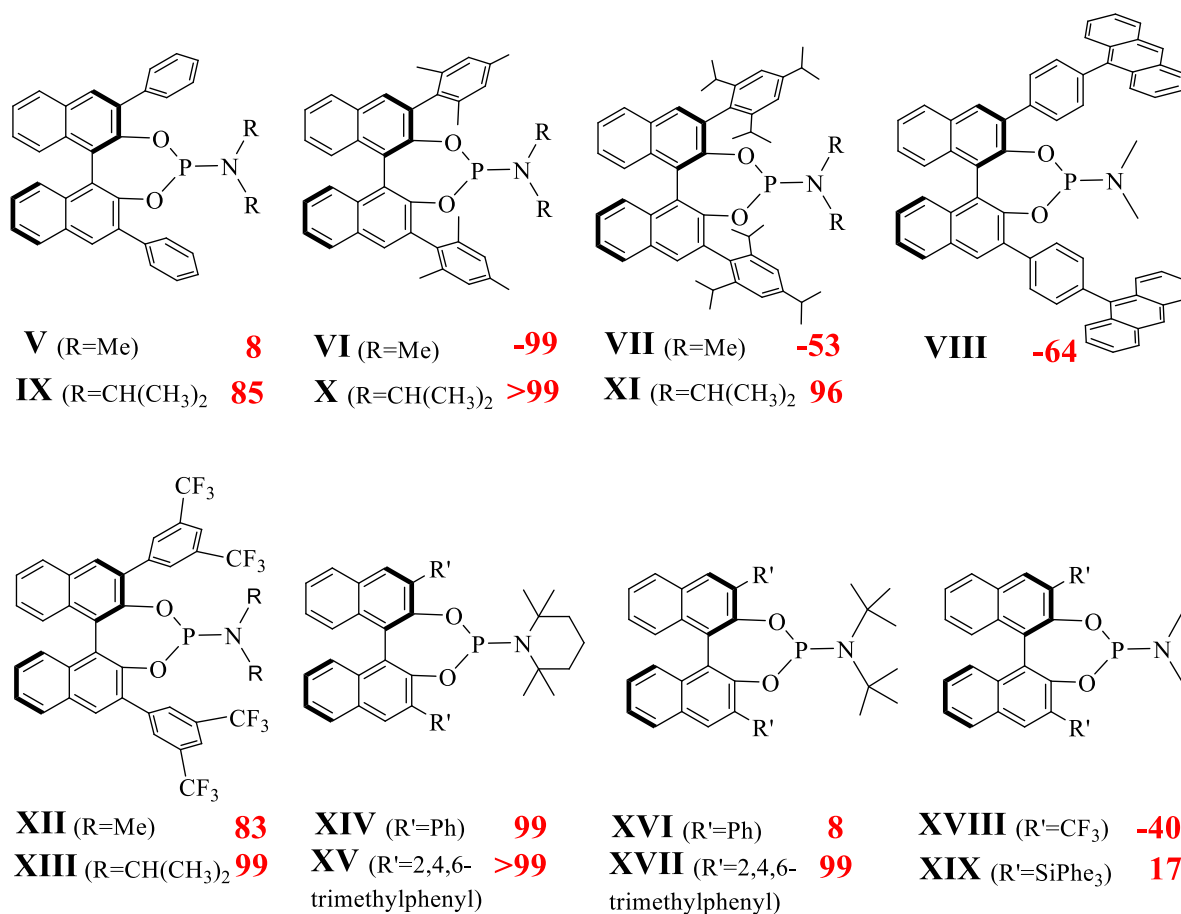


Figure 4. The predicted enantiomeric excess (%*ee*) in Pd-catalyzed asymmetric diamination reaction for different chiral phosphoramidite ligands.

The introduction of different aryl groups at the 3,3' positions of the binol framework gives rise to catalysts **V-XIX**. In the lowest energy TSs of catalysts **I-III**, the C-H $\cdots\pi$ interaction between the C-H of diene and the π -face of binol is noticeable as shown in Figure 3. Similar to the other weak interactions such as an anagostic and C-H \cdots O, the C-H $\cdots\pi$ interactions also play an important role in governing the stereochemical outcome. A representative set of transition states for catalyst **V** is described in more detail here. The geometry of the stereocontrolling transition state for the *si*-face addition of the diene in the case of catalyst **V** reveals the presence

of additional C–H \cdots π interactions (2.90 Å and 3.12 Å) between the diene and the 3-phenyl group of the binol (**V-*si*** in Figure 5). In the absence of phenyl groups at the 3,3' position, such an interaction is not likely. This interaction is further confirmed using the topological analysis of the electron density using the AIM formalism. The ρ_{bcp} values are found to be 0.005 and 0.003 a.u. for the two C–H \cdots π interactions in TS **V-*si*** as shown Figure 5. Obviously, such additional stabilization offered by C–H \cdots π interactions will be absent in those catalysts that lack 3,3'-aryl substituents on the binol backbone (e.g., **I – IV**). In view of this lead, we thought of extending the aryl arm to examine whether a modulation of such interactions could be exploited to steer the facial preferences of the approaching diene.

Encouraged by these insights, the effect of different modified aryl substituents on the enantiomeric excess is examined next. The additional C–H \cdots π interaction is enhanced by the introduction of methyl groups in catalyst **V**, leading to catalyst **VI**. An inversion of enantioselectivity in favor of the *S* isomer is noticed (-99% *ee*) with catalyst **VI**. Further elaboration of the alkyl substituents by introducing 2,4,6-triisopropyl phenyl group (as in **VII**) interestingly resulted in reduction of *ee* to -53%. The increased steric bulk on the binol fragment somewhat counterbalances the effect of weak C–H \cdots π interactions. An interesting observation at this juncture relates to the effect of an extended aromatic arm, such as that in catalyst **VIII**, in affecting the transition state energy ordering. A preference for the approach of the *si*-face of the diene responsible for the formation of the *S* enantiomer is identified in **VIII** (-64%).

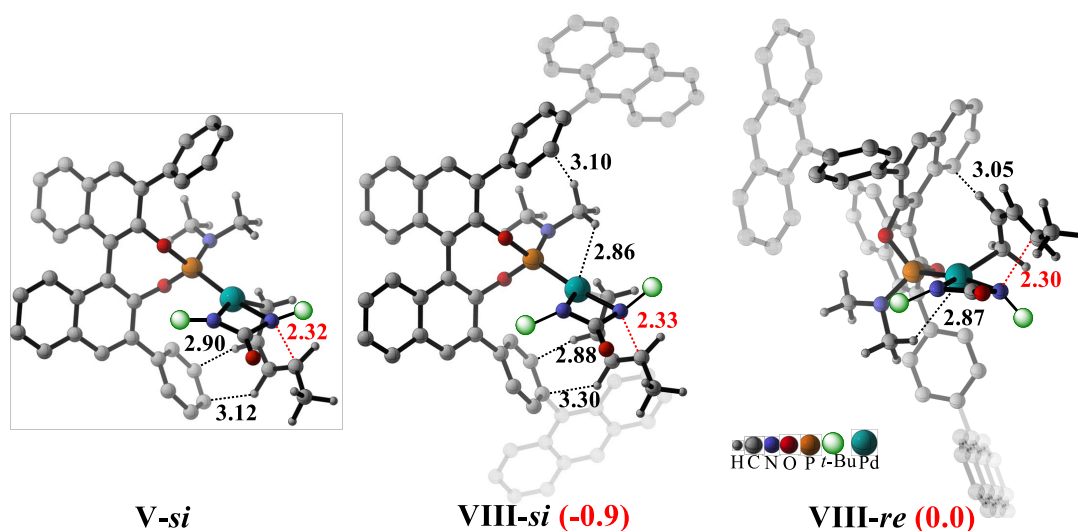


Figure 5. Optimized geometries of the lower energy stereocontrolling transition states for representative catalysts **V** and **VIII**. The relative free energies (in kcal/mol) are given in parenthesis. All distances are in Å.

More prominent C–H $\cdots\pi$ interactions, as compared to the other catalysts hitherto examined, are identified in the case of catalyst **VIII**. The optimized geometries of the diastereomeric TSs (**VIII-*re*** and **VIII-*si***) as shown in Figure 5 conveys the C–H $\cdots\pi$ interactions (a) between the diene and the bridging phenyl group (2.88 Å), and (b) the amido methyl C–H groups and the binol framework (3.10 Å). The former interaction is slightly more pronounced in TS **VIII-*si*** as compared to that in the higher energy **VIII-*re***. These weak interactions are further characterized using the AIM calculations. The ρ_{bcp} values are found to be 0.005 and 0.002 a.u. respectively for the C–H $\cdots\pi$ interactions with the contact distances of 2.88 Å and 3.30 Å in TS **VIII-*si*** (Figure 5). In the higher energy TS **VIII-*re***, destabilizing steric interactions of the *tert*-butyl group of the diaziridinone with the anthracenyl group on the binol backbone are also noticed. The cumulative effect of these interactions leads to an inversion in favour of the *S* enantiomer. These stereoelectronic features of the transition state suggest that suitable

modifications to the 3,3'-aryl substituents as noted in **VI**, **VII** and **VIII** can help invert the stereoselectivity in asymmetric diamination reactions.

The implications of this result could as well be applicable to other asymmetric reactions involving Pd-phosphoramidites. In fact, inversion in stereoselectivity upon changing the 3,3' substituents on chiral binol based phosphoric acids has been earlier reported for a Biginelli reaction²⁸ and aza Friedel-Crafts reaction.²⁹ Other substituents such as CF₃ (**XVIII**), and SiPh₃ (**XIX**) at the 3,3' position failed to improve the *ee*.

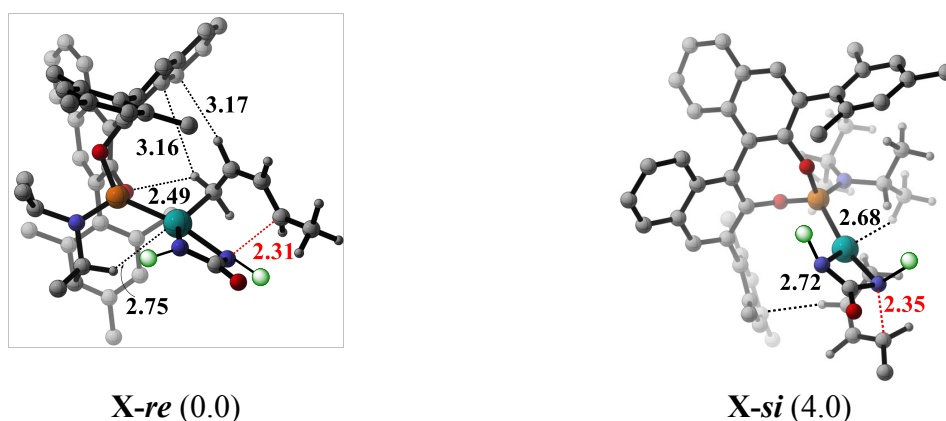


Figure 6. Optimized geometries of the lower energy stereocontrolling transition states for representative catalyst **X**. The relative energies (in kcal/mol) in each case are given in parenthesis. All distances are in Å. Select hydrogens are removed for clarity.

Next, we examined how the modifications on catalyst **II** would influence the enantioselectivity. Catalyst **II** is another experimentally reported catalyst (*ee* = 73%) bearing isopropyl groups on the amido nitrogen. The effect of modifications on the 3,3' substituents of the binol, as shown in **IX** – **XI**, is evaluated (Figure 4). The introduction of phenyl groups (catalyst **IX**) results in a modest increase in the *ee* from 73% to 85%. Further modulation of the steric bulk on the phenyl groups, by using methyl (**X**) or isopropyl (**XI**) substitution, enhances the *ees* to the order of 99% and 96% respectively. A combination of increased distortion and weaker interaction

in the higher energy TS can be regarded as the origin of the energy difference of 4.0 kcal/mol between the diastereomeric TSs for catalyst **X**.³⁰

In the case of substituted piperidines (such as those in catalyst **I** family), the introduction of phenyl groups at the 3,3' positions appears to offer little impact on the predicted *ee*. For instance, the *ees* for **I** and **XIV** are respectively >99 and 99%. The introduction of trimethyl phenyl groups (**XV**) also results in >99% *ee*. Interestingly, di-*tert*-butyl amido together with unsubstituted phenyl groups on binol (**XVI**) yields *ee* of only 8%. Again, the introduction of 2,4,6-trimethyl phenyl groups as in **XVII** is found to offer significant improvements in the *ee* (99%). It appears increasingly more evident that an optimum combination of steric bulk on the amido nitrogen in conjunction with modifications of the 3,3'-aryl substituents on the binol backbone can yield the best catalysts (e.g., **X**, **XV**, **XVII**). Lowering the size of the amido substituents demands increased bulk on the binol while lowering the size on the binol demands increased bulk on the amido to be able to impart higher degree of stereoselectivity.

Now, the role of different substituents on the amido nitrogen such as in catalysts **XX** – **XXVII** is examined (Figure 7). As a natural progression, the effect of *tert*-butyl group with an unsubstituted binol is considered first (**XXI**). The lowest energy TS **XXI-re** consisting of di-*tert*-butyl amido group is found to exhibit stronger anagostic and C–H \cdots π interactions than in the corresponding TSs for catalysts **II** and **III** (Figure 8). Consequently, catalyst **XXI** offers higher *ee* (89%) than for catalysts **II** (73%) and **III** (64%). Although the weak interactions are stronger in **XXI**, prominent steric interaction between the *tert*-butyl groups on the amido nitrogen and diaziridinone in TS **XXI-re** results in lower *ee* than that noticed for catalyst **I** (>99%).

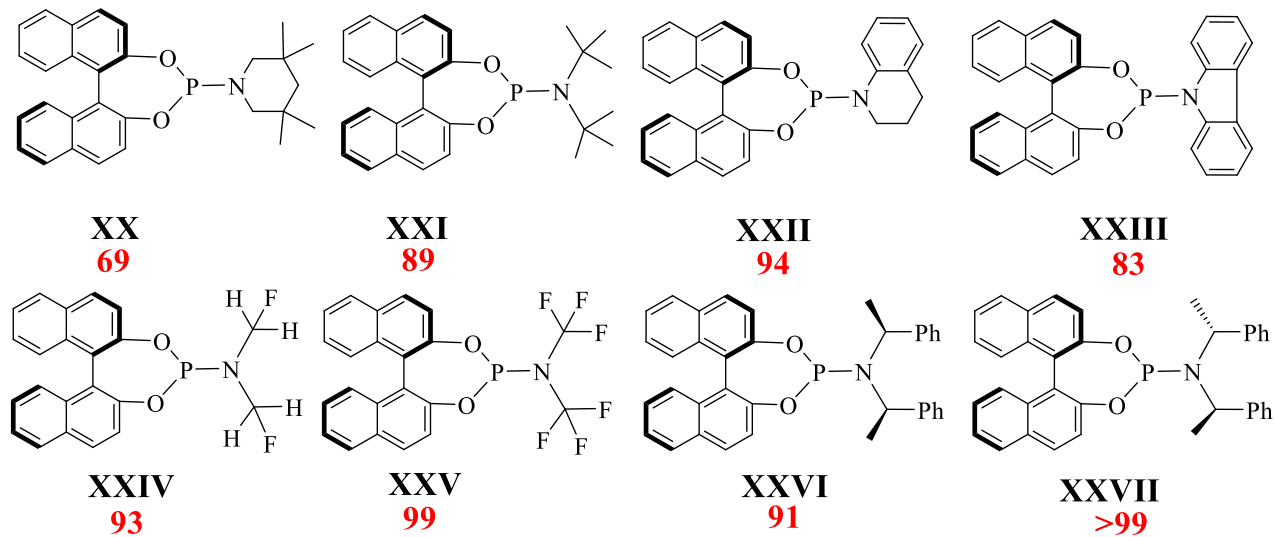


Figure 7. The predicted enantiomeric excess (%*ee*) in Pd-catalyzed asymmetric diamination reaction for different chiral phosphoramidite ligands bearing different amido substituents.

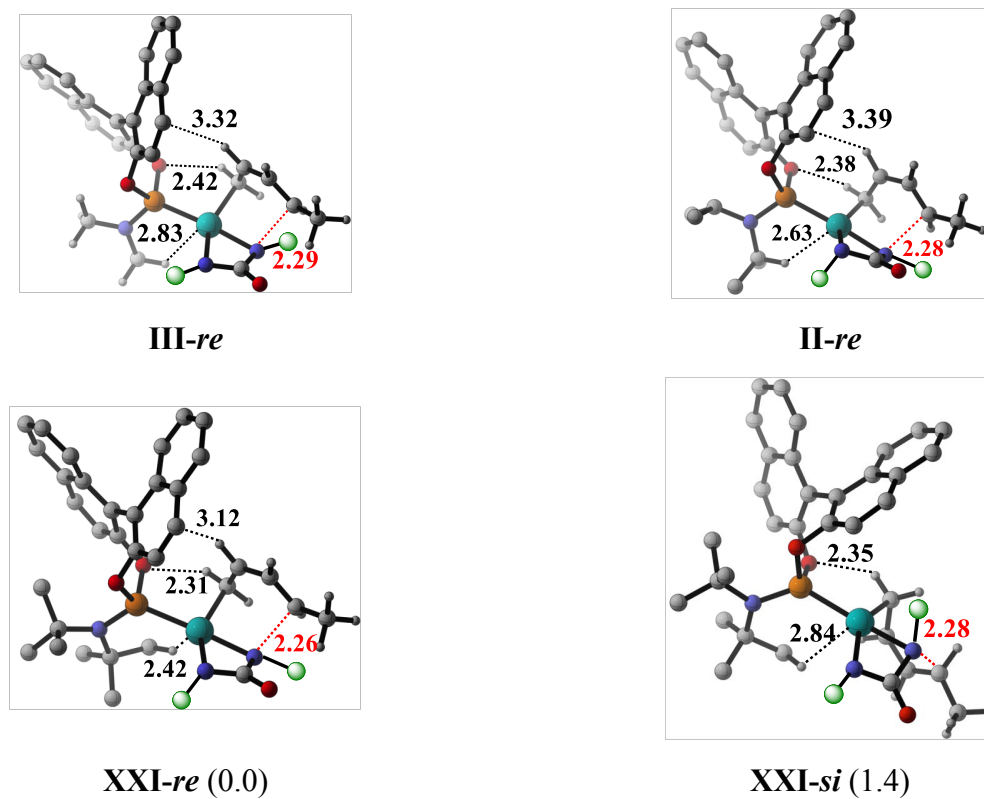


Figure 8. Optimized geometries of lowest energy TSs for methyl, isopropyl and *tert*-butyl groups at amido part. All distances are in Å. The relative energies for XXI are given in parenthesis

Aided by the key insight that improved steric bulk of the substituents on the amido nitrogen is vital to the stereoselectivity, we have investigated the role of substituents at both α and β positions with respect to the nitrogen. The β gem-dimethyl group (**XX**) is found to be less effective than the α gem-dimethyl substitution (**I**). The computed %*ees* for **XX** and **I** are respectively found to be 69 and >99% (%*ee*_{expt} = 91). In the lower energy TS **XX-re**, the C–H \cdots π is absent while anagostic interaction is found to be weaker (Figure 9). Further, the steric bulk at the β position prevents the diene and the binol to come closer so as to allow weak C–H \cdots π interactions in **XX-re**. Also the anagostic interaction distance is longer (2.84 Å) than what is found in the case of α substituent (2.62 Å in **I-re**) (Figure 9). This result suggests that the nature of the substituent at the α -position is quite critical and appears to be a hot spot for modifications.



Figure 9. Optimized geometries of stereodetermining TSs for different catalysts. The relative energies are given in parenthesis. All distances are in Å.

On the basis of these findings, we have subsequently examined the role of electronically active groups such as CH₂F (**XXIV**) and CF₃ (**XXV**) on the amido nitrogen. A large increase in the *ee* with respect to that of catalyst **III** is noticed (Figure 7). Both the position and nature of the amido substituents should therefore be regarded as capable of increasing the energy separation

between the diastereomeric transition states, leading to an overall improvement in the *ee* of the reaction.

Lastly, the role of additional chiral elements such as chiral centers in the amido arms is examined. Catalyst **IV** with an *SS* configuration of the two chiral centers is predicted to yield 95% *ee*, which is in good agreement with the experimental value of 90%. Inversion of one of the chiral centers, as in **XXVI**, did not bring any major difference to the extent or sense of enantioselectivity, with the *ee* being 91% (Figure 7). In the higher energy TS **XXVI-*si***, steric interactions between the *tert*-butyl group of diaziridinone and the methyl group on the chiral center are noticed. Stronger C–H \cdots O and anagostic interactions in the lower energy TS **XXVI-*re*** are found to render additional stabilization (Figure 10). Further calculations with the *RR* isomer (**XXVII**) offers high *ee* of >99%. In summary, additional chirality on the amido arm does not play a direct role in asymmetric diamination, as opposed to other reactions such as Cu-catalyzed conjugate addition with dialkyl Zn reagents and Ir-catalyzed allylic substitution, where only a particular diastereomer of the catalyst results in selectivity.³¹

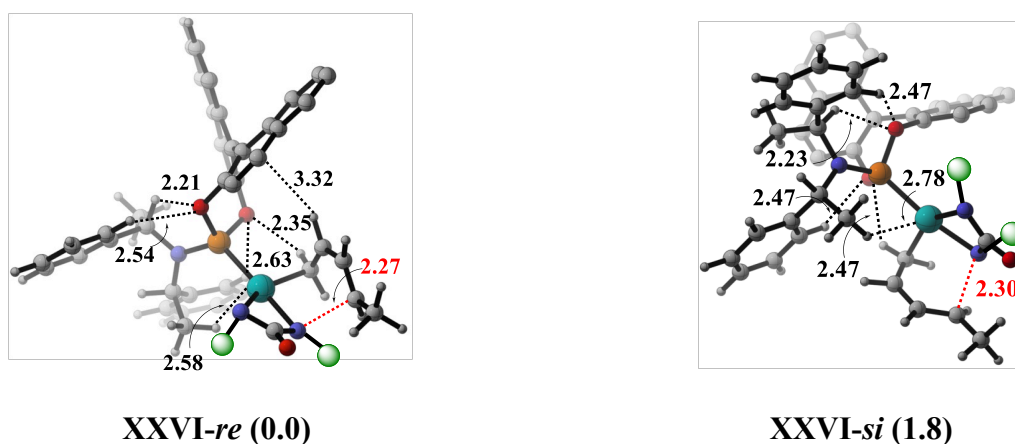


Figure 10. Optimized geometries of lowest energy transition states for catalyst **XXVII**. In parenthesis is given the relative energy (kcal/mol). All distances are in Å.

Table 2. Calculated %*ee* at the M06/6-31G**,LANL2DZ(Pd)//B3LYP/6-31G*,LANL2DZ(Pd) Level of Theory for Catalysts V-XXVII

Catalyst	Calculated % <i>ee</i>	Catalyst	Calculated % <i>ee</i>	Catalyst	Calculated % <i>ee</i>
V	8	XIII	99	XXI	89
VI	-99	XIV	99	XXII	94
VII	-53	XV	>99	XXIII	83
VIII	-64	XVI	8	XXIV	93
IX	85	XVII	99	XXV	99
X	>99	XVIII	-40	XXVI	91
XI	96	XIX	17	XXVII	>99
XII	83	XX	69	-	-

Conclusion

In conclusion, we have designed catalysts for asymmetric diamination, with *ees* greater than 99% by using insights derived from the stereocontrolling transition states (Table 2).³² Subtle and rational modifications to the existing catalysts have provided thirteen new catalysts with a predicted *ee* of 90% or higher. A suitable choice of substituents at the binol and amido group is found to be necessary toward achieving high stereoselectivity. The modulation of C-H \cdots π interactions by suitably changing the groups at the 3,3' position of the binol can even help invert the stereoselectivity. Enhancing the steric bulk at the binol is found to be very effective in obtaining high *ees*. The computational design of catalysts in the present study will not only be useful in the burgeoning field of asymmetric diamination, but the molecular insights would help contribute to the developments in chiral phosphoramidite catalyzed asymmetric reactions.

Acknowledgment Research funding from BRNS (Mumbai), computing time from computer center (IITB) and National Nanotechnology Infrastructure Network (NNIN) at Michigan as well as senior research fellowship (G.J.) from CSIR (New Delhi) are gratefully acknowledged.

Electronic Supplementary Information: Full computational details, optimized Cartesian coordinates of all the transition states, total electronic energies, details of conformational analysis etc., are provided. This material is available free of cost via the Internet at <http://pubs.acs.org>

References

(1) (a) T. P. Yoon and E. N. Jacobsen, *Science*, 2003, **299**, 1691; (b) A. Pfaltz and W. J. Drury III, *Proc. Nat. Acad. Sci. USA*, 2004, **101**, 5723; (c) R. R. Knowles and E. N. Jacobsen, *Proc. Natl. Acad. Sci. U.S.A.*, 2010, **107**, 20678.

(2) K. N. Houk and P. H.-Y. Cheong, *Nature*, 2008, **455**, 309.

(3) (a) D. Rothlisberger, O. Khersonsky, A. M. Wollacott, L. Jiang, J. DeChancie, J. Betker, J. L. Gallaher, E. A. Althoff, A. Zanghellini, O. Dym, S. Albeck, K. N. Houk, D. S. Tawfik and D. Baker, *Nature*, 2008, **453**, 190; (b) J. B. Siegel, A. Zanghellini, H. M. Lovick, G. Kiss, A. R. Lambert, St. J. L. Clair, J. L. Gallaher, D. Hilvert, M. H. Gelb, B. L. Stoddard, K. N. Houk, F. E. Michael and D. Baker, *Science*, 2010, **329**, 309; (c) K. J. H. Young, J. Oxgaard, D. H. Ess, S. K. Meier, T. Stewart, W. A. Goddard and R. A. Periana, *Chem. Commun.*, 2009, **22**, 327; (d) J. DeChancie, F. R. Clemente, A. J. T. Smith, H. Gunaydin, Y.-L. Zhao, X. Zhang and K. N. Houk, *Protein Science*, 2007, **16**, 1851.

(4) (a) P. H.-Y. Cheong, C. Y. Legault, J. M. Um, N. Çelebi-Ölçüm and K. N. Houk, *Chem. Rev.*, 2011, **111**, 5042; (b) H. Yang and M. W. Wong, *J. Org. Chem.*, 2011, **76**, 7399; (b) Y. Wang, J. Wang, J. Su, F. Huang, L. Jiao, Y. Liang, D. Yang, S. Zhang, P. A. Wender and Z.-X. Yu, *J. Am.*

Chem. Soc., 2007, **129**, 10060; (c) S. T. Schneebeli, M. L. Hall, R. Breslow and R. Friesner, *J. Am. Chem. Soc.*, 2009, **131**, 3965; (d) J. M. Brown and R. J. Deeth, *Angew. Chem. Int. Ed.*, 2009, **48**, 4476.

(5) D. Seebach, U. Grošelj, D. M. Badine, W. B. Schweizer and A. K. Beck, *Helv. Chim. Acta*, 2008, **91**, 1999.

(6) (a) C. B. Shinisha and R. B. Sunoj, *Org. Biomol. Chem.*, 2007, **5**, 1287; (b) E. M. Fleming, C. Quigley, I. Rozas and S. J. Connon, *J. Org. Chem.*, 2008, **73**, 948; (c) J. C. Ianni, V. Annamalai, P.-W. Phuan and M. C. Kozlowski, *Angew. Chem. Int. Ed.*, 2006, **45**, 5502; (d) S. Mitsumori, H. Zhang, P. H.-Y. Cheong, K. N. Houk, F. Tanaka and C. F. Barbas III, *J. Am. Chem. Soc.* 2006, **128**, 1040; (e) D. Janardanan and R. B. Sunoj, *J. Org. Chem.*, 2007, **72**, 331; (f) C. B. Shinisha and R. B. Sunoj, *Org. Lett.* 2009, **11**, 3242; (g) K. C. Harper and M. S. Sigman, *Science*, 2011, **333**, 1875; (h) K. C. Harper, E. N. Bess and M. S. Sigman, *Nat. Chem.*, 2012, **4**, 366; (i) K. B. Lipkowitz and M. C. Kozlowski, *Synlett*, 2003, 1547; (j) M. C. Kozlowski and M. Panda, *J. Org. Chem.* 2003, **68**, 2061; (k) T. Dudding and K. N. Houk, *Proc. Nat. Acad. Sci. USA*, 2004, **101**, 5770.

(7) Z.-X. Yu, P. H.-Y. Cheong, P. Liu, C. Y. Legault, P. A. Wender and K. N. Houk, *J. Am. Chem. Soc.*, 2008, **130**, 2378.

(8) P. H.-Y. Cheong and K. N. Houk, *Synthesis*, 2005, **9**, 1533.

(9) (a) P. H.-Y. Cheong, H. Zhang, R. Thayumanavan, F. Tanaka, K. N. Houk and C. F. Barbas III, *Org. Lett.*, 2006, **8**, 81; (b) A. Armstrong, Y. Bhonoah and A. J. P. Colorless, *J. Org. Chem.*, 2009, **74**, 5041.

(10) R. P. Muller, D. M. Philipp and W. A. Goddard III, *Top. Catal.*, 2003, **23**, 81; (b) X. Xu, J. Kua, R. A. Periana and W. A. Goddard III, *Organometallics*, 2003, **22**, 2057.

- (11) (a) F. Proutiere and F. Schoenebeck, *Angew. Chem. Int. Ed.*, 2011, **50**, 8192; (b) F. Proutiere and F. Schoenebeck, *Synlett* 2012, **23**, 645.
- (12) (a) C. B. Shinisha and R. B. Sunoj, *J. Am. Chem. Soc.*, 2010, **132**, 12319; (b) A. K. Sharma and R. B. Sunoj, *Angew. Chem. Int. Ed.*, 2010, **49**, 6373; (c) A. K. Sharma and R. B. Sunoj, *Chem. Commun.*, 2011, **47**, 5759.
- (13) G. Jindal and R. B. Sunoj, *Chem. Eur. J.*, 2012, **18**, 7045.
- (14) (a) F. A. Cardona and A. Goti, *Nature Chem.*, 2009, **1**, 269; (b) R. M. de Figueiredo, *Angew. Chem. Int. Ed.*, 2009, **48**, 1190.
- (15) (a) D. Lucet, T. L. Gall and C. Mioskowski, *Angew. Chem. Int. Ed.*, 1998, **37**, 2580; (b) S. R. S. S. Kotti, C. Timmons and G. Li, *Chem. Biol. Drug Des.*, **2006**, *67*, 101; (c) J.-C. Kizirian, *Chem. Rev.*, 2008, **108**, 140.
- (16) H. Du, B. Zhao and Y. Shi, *J. Am. Chem. Soc.*, 2007, **129**, 11688.
- (17) (a) J. F. Teichert and B. L. Feringa, *Angew. Chem. Int. Ed.*, 2010, **49**, 2486; (b) A. J. Minnaard, B. L. Feringa, L. Lefort and J. G. de Vries, *Acc. Chem. Res.*, 2007, **40**, 1267.
- (18) (a) For more details see ESI. (b) All calculations were performed using Gaussian09 suite of programs. M. J. Frisch, *et al.* Gaussian 09 Revisions A.02 and D.01; Gaussian, Inc.: Wallingford, CT, 2004. See ESI for complete citation.
- (19) (a) W. J. Hehre, R. Ditchfield and J. A. Pople, *J. Chem. Phys.*, 1972, **56**, 2257; (b) P. C. Hariharan and J. A. Pople, *Theor. Chim. Acta*, 1973, **28**, 213; (c) C. Lee, W. Yang and R. G. Parr, *Phys. Rev. B*, 1988, **37**, 785; (d) A. D. Becke, *J. Chem. Phys.* 1993, **98**, 5648; (e) Y. Zhao and D. G. Truhlar, *Theo. Chem. Acc.*, 2008, **120**, 215; (f) Y. Zhao and D. G. Truhlar, *Acc. Chem. Res.*, 2008, **41**, 157; (g) Y. Zhao and D. G. Truhlar, *Org. Lett.*, 2007, **9**, 1967.
- (20) P. J. Hay and W. R. Wadt, *J. Chem. Phys.*, 1985, **82**, 299.

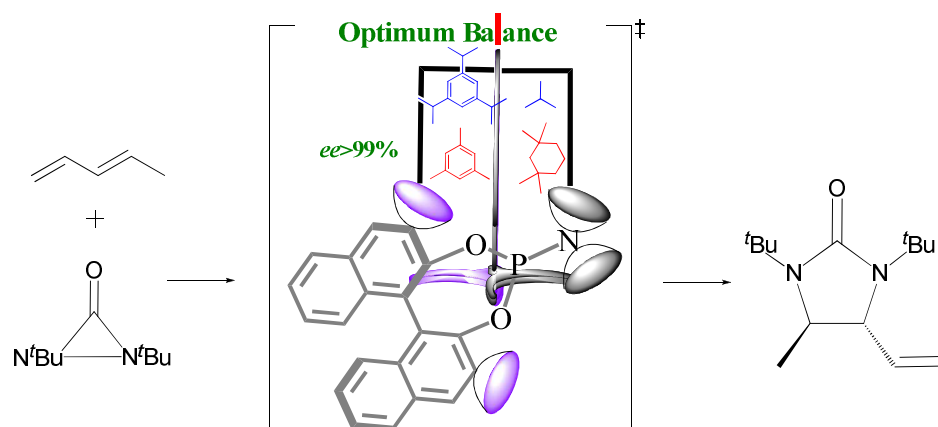
-
- (21) S. Grimme, *J. Comput. Chem.*, 2006, **27**, 1787.
- (22) (a) R. F. Bader, *Atoms in Molecules: A Quantum Theory*; Clarendon Press: Oxford, 1990; (b) *AIM2000 Version 2.0*; Buro fur Innovative Software, SBK-Software: Bielefeld, Germany, 2002; (c) F. Biegler-Konig, J. Schonbohm and D. Bayles, *J. Comput. Chem.*, 2001, **22**, 545; (d) F. Biegler-Konig and J. Schonbohm, *J. Comput. Chem.*, 2002, **23**, 1489.
- (23) (a) J. Ran and M. W. Wong, *J. Phys. Chem. A*, 2006, **110**, 9702; (b) J. J. Novoa and F. Mota, *Chem. Phys. Lett.*, 2000, **318**, 345; (c) S. J. Grabowski and P. Lipkowski, *J. Phys. Chem. A*, 2011, **115**, 4765; (d) M. Kumari, P. V. Balaji and R. B. Sunoj, *Phys. Chem. Chem. Phys.*, 2011, **13**, 6517; (e) The topological map generated using the AIM analyses depicting the bond paths as well as bond critical points are provided in the ESI in Figure S1.
- (24) The details of an extensive conformational analysis is provided in Tables S1-S4 in the ESI.
- (25) E. H. Krenske, K. N. Houk, A. G. Lohse, J. E. Antoline and R. P. Hsung, *Chem. Sci.*, 2010, **1**, 387.
- (26) W. Zhang, Y. Zhu, D. Wei, Y. Li and M. Tang, *J. Org. Chem.*, 2012, **77**, 10729.
- (27) For reactions with bulky substituents at 3,3' position of binol, See: (a) I. Alonso, B. Trillo, F. López, S. Montserrat, G. Ujaque, L. Castedo, A. Lledós and J. L. Mascarénas, *J. Am. Chem. Soc.* 2009, **131**, 13020; (b) A. Z. González, D. Benitez, E. Tkatchouk, W. A. Goddard III and F. D. Toste, *J. Am. Chem. Soc.* 2011, **133**, 5500; (c) L. Wang, W. Meng, C.-L. Zhu, Y. Zheng, J. Nie and J.-A. Ma, *Angew. Chem. Int. Ed.*, 2011, **50**, 9442; (d) A short compilation of phosphoramidites are provided in Table S7 in ESI.
- (28) X.-H. Chen, X.-Y. Xu, H. Liu, L.-F. Cun and L.-Z. Gong, *J. Am. Chem. Soc.*, 2006, **128**, 14802.

(29) M. Terada, S. Yokoyama, K. Sorimachi and D. Uraguchi, *Adv. Synth. Catal.*, 2007, **349**, 1863.

(30) The *Distortion-Interaction* model is applied to examine the origin of the energy difference between the stereodetermining TSs, **X-re** and **X-si**. For more details see page S14 of ESI. See: (a) F. M. Bickelhaupt, *J. Comput. Chem.*, 1999, **20**, 114; (b) A. Diefenbach and F. M. Bickelhaupt, *J. Phys. Chem. A*, 2004, **108**, 8460; (c) G. T. de Jong, R. Visser and F. M. Bickelhaupt, *J. Organomet. Chem.*, 2006, **691**, 4341; (d) C. Y. Legault, Y. Garcia, C. A. Merlic and K. N. Houk, *J. Am. Chem. Soc.*, 2007, **129**, 12664.

(31) (a) B. L. Feringa, M. Pineschi, L. A. Arnold, R. Imbos and A. H. M. de Vries, *Angew. Chem. Int. Ed.*, 1997, **36**, 2620; (b) C. A. Kiener, C. Shu, C. Incarvito and J. F. Hartwig, *J. Am. Chem. Soc.*, 2003, **125**, 14272.

(32) %*ee* values obtained at other levels of theory are provided in Table S6 of ESI.



DFT calculations have been used to design chiral phosphoramidite ligands for the asymmetric diamination of vicinal diamines. The substituents at both the 3,3' positions of the binol framework and the amido nitrogen play a vital role in the stereochemical outcome.